ELSEVIER

Available online at www.sciencedirect.com

ScienceDirect

Journal of Catalysis 250 (2007) 128–138

JOURNAL OF CATALYSIS

www.elsevier.com/locate/jcat

Selective oxidation of *n*-butane over MoV-containing oxidic bronze catalysts

B. Solsona, F. Ivars, P. Concepción, J.M. López Nieto *

Instituto de Tecnología Química, UPV-CSIC, Avda. de los Naranjos s/n, 46022 Valencia, Spain

Received 2 January 2007; revised 19 May 2007; accepted 28 May 2007

Abstract

MoV-containing oxidic bronze catalysts were synthesized, characterized, and tested in the selective oxidation of *n*-butane. For comparison, an activated V–P–O catalyst was also studied. The catalytic behavior of MoV-containing catalysts was found to be dependent on both the catalyst composition and the nature of crystalline phases. In this way, the M1 phase (i.e., $Te_2M_{20}O_{57}$ and $(SbO)_2M_{20}O_{56}$ in Te- and Sb-containing catalysts, respectively) is proposed as an active and selective crystalline phase for *n*-butane oxidation on these catalysts. The selectivity to maleic anhydride/acid obtained on MoV-catalysts follows the order: MoVTeNbO > MoVTeO = MoVSbNbO > MoVSbO > MoVNbO. Although less selective than a vanadium phosphorous catalyst, a higher productivity to MA is obtained over a MoVTeNbO mixed oxide catalyst as a consequence of its remarkably superior catalytic activity. Moreover, the amount of maleic anhydride obtained on oxidic bronze catalysts strongly depends on the composition of the feed. In addition, the nature of active sites, the reaction network for *n*-butane oxidation, and a comparison of their catalytic performance in the oxidation of C_2–C_4 alkanes are discussed.

Keywords: *n*-Butane oxidation to maleic anhydride; Propane to acrylic acid; Mo–V–Te–Sb–Nb mixed metal oxides; V–P–O catalyst; FTIR of adsorbed 1-butene

1. Introduction

The gas-phase oxidation of *n*-butane to maleic anhydride with molecular oxygen is a commercial process that uses catalysts based on vanadyl pyrophosphate, $(VO)_2P_2O_7$ (V–P–O) [1–4]. During the last 30 years, hundreds of papers have been devoted to this reaction and this catalytic system; studying the reaction conditions, influence of promoters, new crystalline phases, and structures, and so on [1–4]. Although much is known about VPO catalysts, there is still a large margin for improvement, because the highest yields to maleic anhydride at industrial scale are around 70%. However, at present, there is no alternative catalyst that achieves comparable performance.

V–P–O oxides have shown good catalytic performance in other reactions involving short-chain alkanes, although not as efficient as in the transformation of *n*-butane to maleic anhydride. For example, high yields to maleic anhydride and phthalic anhydride can be obtained during the oxidation of *n*-pentane [5,6] on very active VPO catalysts. Moreover, acrylic acid and ethylene also can be obtained with reasonable productivity during the partial oxidation of propane [7–10] and ethane [11–13], respectively.

In recent studies, Davies et al. [14–17] observed that niobium- and pyridine-exchanged molybdovanadophosphoric acid catalysts give good selectivity to partial oxidation products during the selective oxidation of C_2–C_4 alkanes. Thus, maleic anhydride from *n*-butane [14,15], acrylic acid, and maleic anhydride from propane [14–16] or ethylene acetic acid from ethane [15,17] can be obtained with relatively high selectivity and high activity on these reduced heteropolyanions. These results suggest that the activation of light alkanes occurs by a similar mechanism, as also has been proposed for the oxidative dehydrogenation of C_2–C_4 alkanes [18–20]. However, the nature (and selectivity) of the partial oxidation products depends on both the alkane fed and the physicochemical properties of catalysts.

In the early 1990s, Ushikubo et al. proposed MoVTe(Sb)NbO mixed-metal oxides as a new catalytic system active and selective for the selective (amm)oxidation of propane to acrylonitrile and acrylic acid [21,22]. More recently, these multicomponent catalysts have been reported to be very selective in the oxidative dehydrogenation of ethane to ethylene [23,24]. Typically, the most efficient MoVTe(Sb)NbO catalysts present

---

* Corresponding author. Fax: +34 96 3877809.
E-mail address: jmlopez@itq.upv.es (J.M. López Nieto).

0021-9517/$ – see front matter © 2007 Elsevier Inc. All rights reserved.
doi:10.1016/j.jcat.2007.05.023

at least two crystalline phases [22–34]: (i) an orthorhombic $(AO)_{2-2x}(A_2O)_nM_{20}O_{56}$ (A = Te or Sb and M = Mo, V, Nb, with $0 < x < 1$), the so-called M1, and (ii) an orthorhombically distorted $Te_{0.33}MO_{3.33}$ or $(Sb_2O)M_6O_{19}$ phase (M = Mo, V, Nb), the so-called M2. In addition, $TeMo_5O_{16}$ (or $Sb_4Mo_{10}O_x$), (V, Nb)-containing Mo_5O_{14}, and/or tetragonal bronzes may be present, depending on the catalyst preparation procedure [27,28,33]. However, the M1 phase itself is active and selective on the partial oxidation of propane and ethane [23–33].

V–P–O, partially reduced heteropolyanions, and MoVTe(Sb)NbO catalytic systems are active in the selective oxidative activation of ethane and propane. Therefore, studying the catalytic behavior of MoV-containing oxidic bronze catalysts in the selective oxidation of *n*-butane, in which both VPO and partially reduced heteropolyanions show high selectivity to maleic anhydride, also is of interest.

In the present work, we investigated the catalytic behavior of ternary and quaternary MoVTe(Sb)NbO mixed-metal oxides in the selective oxidation of *n*-butane and 1-butene and compare the results with those obtained on a V–P–O catalyst. In addition, we investigated the reaction network operating during the *n*-butane oxidation on these MoV-based catalysts on the basis of FTIR results on the adsorption of 1-butene over the most efficient catalyst.

2. Experimental

2.1. Catalyst preparation

MoV-containing oxidic bronze catalysts were prepared from slurries containing aqueous solutions of ammonium metavanadate, ammonium heptamolybdate tetrahydrate, telluric acid (or antimony sulfate), and/or niobium oxalate as described previously [34]. The solids obtained were then heat-treated in flowing N_2 at 600 °C for 2 h. The characteristics of these catalysts are summarized in Table 1.

For comparison, a vanadyl pyrophosphate-based catalyst has been prepared as described previously [36]. In short, V_2O_5 (15 g) and H_3PO_4 85 wt% (12.3 ml) were added to isobutanol (320 ml). This mixture was refluxed at 105 °C for 16 h in a N_2 atmosphere. The suspension thus obtained was filtered and washed with isobutanol and ethanol. The solid thus obtained was refluxed in hot water, filtered, and dried in air at 110 °C for 16 h. As suggested in the literature [1–4,36–38], the precursor was activated in *n*-butane oxidation reaction conditions (i.e., *n*-C_4H_{10}/O_2/He molar ratio of 1.5/18.5/80 and a GHSV of 1200 h^{-1}) at 400 °C for 168 h. This precursor is designated VPO-A.

2.2. Catalyst characterization

X-ray diffraction (XRD) patterns were collected using a Phillips X'Pert diffractometer equipped with a graphite monochromator, operating at 40 kV and 45 mA, and using nickel-filtered Cu$K\alpha$ radiation ($\lambda = 0.1542$ nm). Chemical analyses of the catalysts were carried out by atomic absorption (Mo, V, and Te) and ICP (Sb and Nb).

IR spectra of 1-butene adsorption/desorption were recorded with a Bio Rad, FTS-40A FTIR spectrophotometer using a conventional quart IR cell connected to a vacuum dosing system. Before 1-butene adsorption, the samples were evacuated at 250 °C for 2 h and cooled down to room temperature (room temperature) in vacuum (10^{-4} mbar). Adsorption of 1-butene was performed at room temperature, followed by evacuation at the same temperature. IR spectra were collected at room temperature and at increasing temperatures up to 350 °C. Co-adsorption of O_2 also was studied at these temperatures.

2.3. Catalytic tests

The catalytic experiments were performed in a fixed-bed quartz tubular reactor (12 mm i.d., 400 mm long) under atmospheric pressure. The catalyst samples (0.25–2.5 g with a 0.3- to 0.5-mm particle size) and silicon carbide (1–6 g) were introduced into the reactor to maintain a constant volume in the catalytic bed. The flow rate was 25–100 ml/min for *n*-butane oxidation. The reaction temperature was 360–400 °C, focused mainly at 380 °C. The feed comprised a mixture of *n*-butane, oxygen, and helium with a molar ratio of 1.5/18.5/80.

The oxidation of 1-butene or propane also was studied at 300–420 °C. 1-Butene oxidation was carried out at a space velocity of 21,750 h^{-1} (or 7250 h^{-1} in the case of VPO-A catalyst) and a feed comprising 1-C_4H_8/O_2/He at a molar ratio of 1.5/18.5/80. Propane oxidation was carried out using

Table 1
Characteristics of MoV-based catalysts synthesised

Catalyst	Chemical composition[a]	S_{BET} (m^2/g)	Crystalline phases (XRD)	Propane oxidation[b]	
				Conversion (%)[c]	S_{AA} (%)[d]
MN-1	$Mo_1V_{0.23}Nb_{0.14}O_x$	6.4	$Mo_{0.67}V_{0.33}O_2$, $(Mo_{0.93}V_{0.07})_5O_{14}$, $Nb_{0.09}Mo_{0.91}O_{2.8}$	10	0
MS-2	$Mo_1V_{0.18}Sb_{0.15}O_x$	14.5	$(SbO)_2M_{20}O_{56}$, $(SbO)_2M_6O_{19}$	8.5	10
MT-3	$Mo_1V_{0.30}Te_{0.23}O_x$	15.0	$Te_2M_{20}O_{57} > Te_{0.33}MO_{3.33}$, $(Mo_{0.93}V_{0.07})_5O_{14}$	24	23
MSN-4	$Mo_1V_{0.26}Sb_{0.13}Nb_{0.06}O_x$	18.0	$(SbO)_2M_{20}O_{56} \gg (SbO)_2M_6O_{19}$, $(Mo_{0.93}V_{0.07})_5O_{14}$	13	29
MTN-5	$Mo_1V_{0.23}Te_{0.23}Nb_{0.15}O_x$	5.4	$Te_2M_{20}O_{57}$, $Te_{0.33}MO_{3.33}$	24	69
VPO-A	$VP_{1.1}O_x$	12.2	$(VO_2)P_2O_7$	5.0	1

[a] Chemical composition was obtained by atomic absorption spectroscopy.

[b] Oxidation of propane was carried out with a feed consisting of propane/O_2/He/H_2O = 4/8/58/30 (molar ratio).

[c] Propane conversion at 380 °C and a $W/F = 200\ g_{cat}\ h/mol\,C_4$.

[d] Selectivity to acrylic acid obtained at 380 °C and a propane conversion = 20%.

$C_3H_8/O_2/He/H_2O$ at a molar ratio of 4/8/58/30 and a reaction temperature of 380 °C.

Reactants and reaction products were analysed using two chromatographs, an online chromatograph with a thermal conductivity detector containing two chromatographic columns (Molecular Sieve and Porapak Q) to analyse the carbon oxides, oxygen, alkanes, olefins, and oxygenates, and an offline chromatograph with a flame ionization detector equipped with a capillary column (Plot Alumina, 50 m) to provide a better analysis of C_4 olefins. Mass spectrometry also was used to detect minor products.

The blank runs were carried out at a reaction temperature of 400 °C, using a low gas flow (25 ml min^{-1}). No *n*-butane transformation was observed, whereas for 1-butene, an olefin conversion of 1% was observed at 400 °C.

3. Results

3.1. Catalyst characterization

The main characteristics of the catalysts are summarized in Table 1. All of them have low surface areas, although they depend on the chemical composition. Fig. 1 shows the XRD patterns of MoV-containing catalysts, and Table 1 summarizes the main crystalline phases. Except for sample MN-1 (Fig. 1a), the main crystalline phases were $Te_2M_{20}O_{57}$ and $Te_{0.33}MO_{3.33}$ for Te-containing samples and $(SbO)_2M_{20}O_{56}$ and $(Sb_2O)M_6O_{19}$ for Sb-containing samples (M = Mo, V, Nb). In addition to these, $(Mo_{0.93}V_{0.07})_5O_{14}$ (JCPDS: 31-1437) and/or $Nb_{0.09}Mo_{0.91}O_{2.8}$ (JCPDS: 27-310) appeared as minor products in Nb-containing catalysts. In the case of MN-1 catalyst, the XRD pattern suggests the presence of $Mo_{0.67}V_{0.33}O_2$, $(Mo_{0.93}V_{0.07})_5O_{14}$, $Nb_{0.09}Mo_{0.91}O_{2.8}$.

The XRD pattern of VPO-A catalyst shown in Fig. 1 (pattern f), is typical of $(VO)_2P_2O_7$ (JCPDS: 41-698), similar to those reported for active and selective V–P–O catalysts [1–6, 35,36].

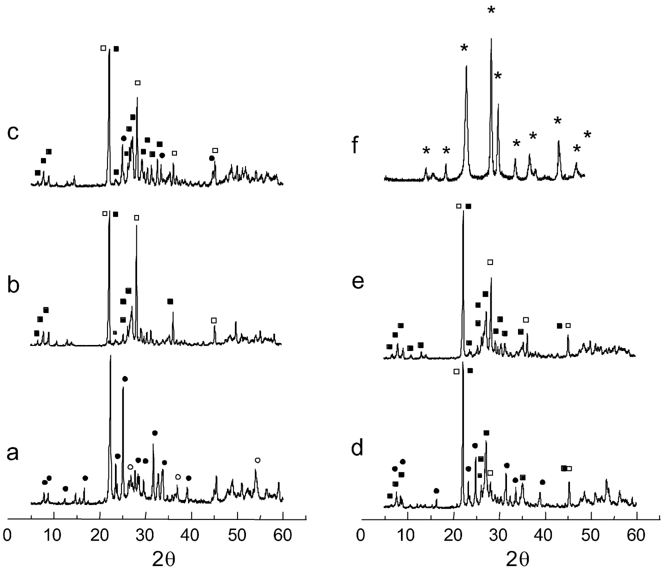

Fig. 1. XRD patterns of calcined in N_2 at 600 °C MoV-containing catalysts: (a) MoVNb, (b) MS-2, (c) MT-3, (d) MSN-4, (e) MTN-5. For comparison, the XRD pattern of VPO-A sample after activation in *n*-butane/oxygen fed is also included (f). Symbols: (■) M1-type phases $Te_2M_{20}O_{57}$ or $(Sb_2O)_2M_{20}O_{56}$, (□) M2-type phases $Te_{0.33}MO_{3.3}$ or $(Sb_2O)M_6O_{19}$, (●) $(V_{0.07}Mo_{0.93})_5O_{14}$ or $Nb_{0.09}Mo_{0.91}O_{2.8}$, (○) $V_{0.33}Mo_{0.67}O_2$; (∗) $(VO)_2P_2O_7$.

3.2. Catalytic tests for *n*-butane oxidation

Table 2 compares the results obtained from the oxidation of *n*-butane over MoV-containing oxidic bronze catalysts and over a VPO-A catalyst. Fig. 2 shows the variation in the selectivity to maleic anhydride with the *n*-butane conversion obtained over MoV-containing catalysts. Maleic anhydride, CO, and CO_2 are the main reaction products in the oxidation of *n*-butane over MoV-based catalysts. Acrylic acid, acetic acid, 2-butenes (*trans*- and *cis*-2-butene), and butadiene also were detected, whereas methoxy acetic acid, phthalic anhydride, and acetone were only minor products. Except for the MoVNbO mixed oxide (sample MN-1), the catalysts studied here are active and relatively selective in the formation of maleic anhydride from *n*-butane. Also note that the selectivity to maleic anhydride is almost constant in the range of alkane conversions studied here (up to 60%), suggesting that the maleic anhydride thus formed has high stability to overoxidation. These results, shown in Fig. 2 and Table 2, indicate that both the catalytic activity and selectivity to maleic anhydride depend strongly on the catalyst composition and that the selectivity to maleic anhy-

Table 2
Oxidation of *n*-butane over MoV-containing catalysts[a]

Catalyst	GHSV (h^{-1})	Conversion (%)	Selectivity (%)[b]						STY_{MA}[c]
			MA	AA	AcOH	$C_4^=$	CO_2	CO	
MN-1	4350	45.5	0	0	0	1.0	58.8	40.2	0
MS-2	4350	37.8	7.4	0	0.4	1.6	48.4	41.6	5.0
MT-3	4350	54.4	25.6	0.2	0.2	0.8	32.5	40.6	24.9
MSN-4	4350	56.5	24.7	0.3	0.2	1.0	33.4	40.1	25.0
MTN-5	4350	56.2	35.9	1.2	0	0.7	29.2	32.6	36.4
VPO-A	1200	58.7	66.2	0	0	0	15.3	18.6	19.5

[a] Reaction conditions: 1.5% *n*-C_4H_{10}/air, $T = 400$ °C.

[b] Selectivity to the main reaction products: maleic anhydride (MA); acrylic acid (AA); acetic acid (AcOH); C_4-olefins and diolefins ($C_4^=$). Other reaction products observed: phthalic anhydride, methoxy acetic acid, acetone.

[c] Rate of formation of maleic anhydride per unit mass of catalyst per unit time, STY_{MA}, in $g_{MA}\,h^{-1}\,kg_{cat}^{-1}$.

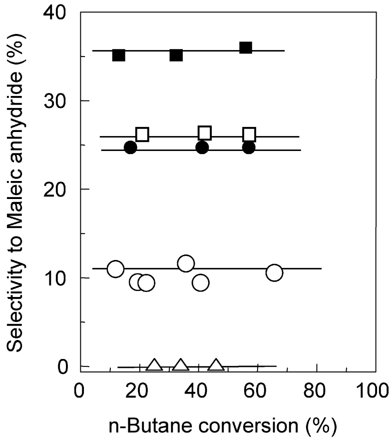

Fig. 2. Variation of the selectivity to maleic anhydride with the *n*-butane conversion obtained during the *n*-butane oxidation at 380 °C for MoV-containing catalysts: (△) MN-1, (○) MS-2, (□) MT-3, (●) MSN-4, (■) MTN-5. Reaction conditions in text.

dride decreases in the following order: MTN-5 (36%) > MT-3 (26%) = MSN-4 (25%) > MS-2 (7%) > MN-1 (0%).

The catalytic results obtained on an activated V–P–O catalyst (sample VPO-A), also given in Table 2, are similar to those previously reported by other authors with selectivity to maleic anhydride ranging from 60 to 80% [1–6]. Although with a significantly lower catalytic activity, the VPO-A sample shows higher selectivity to maleic anhydride than any of the MoV-based catalyst, as well as less byproduct formation. In fact, only carbon oxides were detected by gas chromatography as byproducts (although very small amounts of acetic acid and phthalic anhydride were detected by mass spectrometry). Nevertheless, because of the large difference in reactivities, the rate of maleic anhydride formation per unit mass of catalyst per unit time, STY_{MA}, obtained on a MoVTeNbO mixed-oxide catalyst (sample MTN-5) was ca. twice that obtained over the VPO-A catalyst (Table 2).

Table 3 gives the catalytic results obtained during *n*-butane oxidation over MTN-5 catalyst using different *n*-butane/oxygen ratios. Note that to avoid the total consumption of the molecular oxygen, we used a space velocity of 4350 h^{-1} for O_2-rich feed (n-$C_4/O_2/He$ molar ratios of 1.5/18.5/80 or 4/8/88), whereas we used a higher space velocity (17,400 h^{-1}) in the O_2-poor feed (n-$C_4/O_2/He$ = 8/4/88, molar ratio). The results collected in Table 3 demonstrate that the reaction conditions influence the selectivity to the main reaction products. Thus, the higher the fuel/O_2 ratio, the higher the selectivity to maleic anhydride and the rate of formation of maleic anhydride per unit of mass per unit time (STY_{MA}). Furthermore, high selectivity to C_4-olefins can be observed when working in O_2-poor conditions.

3.3. Oxidation of 1-butene

The oxidation of 1-butene was studied over some representative catalysts: MTN-5, the most efficient MoV-catalyst in *n*-butane oxidation; MS-2, a catalyst poorly selective in *n*-butane oxidation but active in the oxidative scission of C_3-olefin [38]; and VPO-A. Figs. 3 and 4 show the catalytic results obtained from 1-butene oxidation. Note that to obtain similar butane conversions, we used a space velocity of 21,750 h^{-1} in the oxidation of 1-butene on MTN-5 and MS-2 catalysts and used a space velocity of 7250 h^{-1} in the oxidation of 1-butene on VPO-A catalyst, suggesting that VPO-A is less active (about 3 times less active) than MTN-5 or MS-2 catalysts.

For all of the catalysts, the main reaction products were 2-butenes, butadiene, maleic anhydride, and carbon oxides, with acrylic acid, acetic acid, or furane were observed in some cases. Nevertheless, many reaction products were detected up to 20% conversion of 1-butene on all catalysts, in contrast with the few products observed during the oxidation of *n*-butane. This finding has been described by other authors [1–4] and can be explained by the high adsorption of butenes on the catalyst surface with respect to *n*-butane [3].

Fig. 3 shows the variation of 1-butene conversion and the yield of maleic anhydride with the reaction temperature obtained during the oxidation of 1-butene over the three types of catalysts. A maximum yield of maleic anhydride of ca. 40% was achieved over MTN-5 catalyst (Fig. 3b), compared with ca. 20% over MS-2 and ca. 50% over VPO-A at similar 1-butene conversions (Figs. 3a and 3c, respectively).

Fig. 4 illustrates the variation in selectivity to the main partial oxidation products with the reaction temperature obtained during the oxidation of 1-butene on these catalysts. For all catalysts, the selectivity to maleic anhydride increased with the reaction temperature, achieving maximum values of ca. 25%

Table 3
Oxidation of *n*-butane over MVT-5 catalyst. Influence of the feed composition[a]

Feed (molar) n-$C_4/O_2/N_2$	GHSV (h^{-1})	*T* (°C)	Conversion (%)		Selectivity (%)[b]						STY_{MA}[c]
			C_4H_{10}	O_2	MA	AA	AcOH	$C_4^=$	CO_2	CO	
1.5/18.5/80	4350	380	32.7	13.5	35.3	0.6	0.4	1.5	29.5	32.5	20.9
	4350	400	56.2	22.4	35.9	1.2	0	0.7	29.2	32.6	36.4
4/8/88	4350	380	22.8	48.0	42.6	7.5	0.5	4.9	21.8	22.0	46.8
	4350	400	43.1	89.7	42.9	10.3	0.3	2.3	21.0	22.5	89.0
8/4/88	17400	380	3.1	21.7	38.0	0.5	0.1	28.8	17.2	15.3	44.4
	17400	400	10.7	81.2	46.6	1.8	0.1	18.3	15.9	16.6	188

[a] Total flow in all experiments was 50 ml/min.

[b] Selectivity to the main reaction products: maleic anhydride (MA); acrylic acid (AA); acetic acid (AcOH); C_4-olefins and diolefins ($C_4^=$). Other reaction products observed: phthalic anhydride, methoxy acetic acid, acetone.

[c] Rate of formation of maleic anhydride per unit mass of catalyst per unit time, STY_{MA}, in $g_{MA}\ h^{-1}\ kg_{cat}^{-1}$.

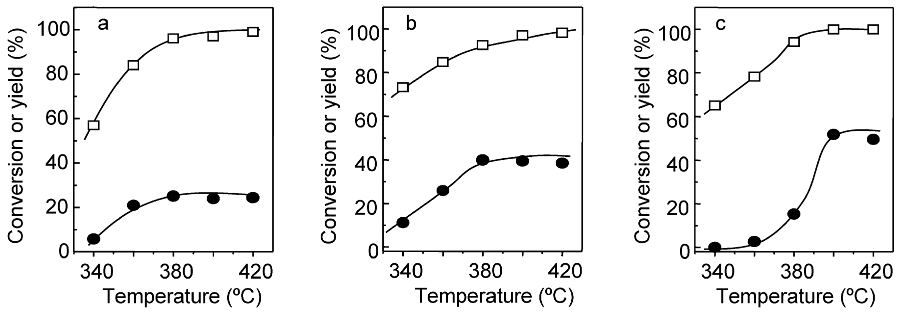

Fig. 3. Variation of the 1-butene conversion (□) and the yield of maleic anhydride (●) with the reaction temperature obtained during the oxidation of 1-butene over (a) MS-2, (b) MTN-5, and (c) VPO-A catalysts. Reaction conditions: 1.5% of hydrocarbon in air, GHSV = 21,750 h^{-1} (GHSV = 7250 h^{-1} for VPO-A catalyst).

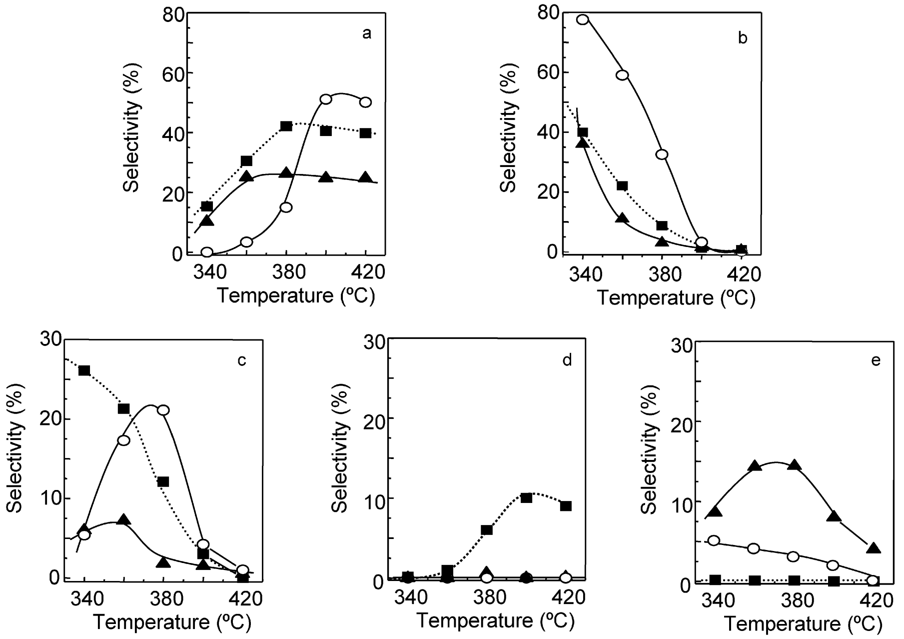

Fig. 4. Variation of the selectivity to main partial oxidation products with the reaction temperature obtained during the oxidation of 1-butene over (▲) MS-2, (■) MTN-5, and (○) VPO-A catalysts: (a) maleic anhydride, (b) 2-butene, (c) butadiene, (d) acrylic acid, (e) acetic acid. Reaction conditions as Fig. 3.

for MS-2, 40% for MTN-5, and 50% for VPO-A (Fig. 4a). Because these results were obtained at similar 1-butene conversions, we can conclude that at low reaction temperatures, maleic anhydride was obtained more easily on MTN-5, whereas at high reaction temperatures, it was obtained more selectively on VPO-A catalyst.

The selectivity to 2-butenes (formed by isomerization of 1-butene) tended to decrease with the reaction temperature (Fig. 4b), indicating that this is a primary and unstable reaction product. Meanwhile, the selectivity to butadiene reached a maximum at 340 °C for MTN-5, at 360 °C for MS-2, and at 380 °C for VPO-A (Fig. 4c), suggesting that butadiene is a secondary and unstable reaction product. The different temperatures observed for the maximum selectivity to butadiene can be explained by the different catalytic activity for 1-butene oxidation of each catalyst. Accordingly, it is very likely that 1-butene, as well as 2-butenes (*cis*- and *trans*-2-butene), react initially to yield butadiene, which is subsequently transformed into maleic anhydride [1–4].

Important differences in the formation of minor products also were observed on these catalysts. For example, acrylic acid was formed at a yield close to 10% (whereas only traces of acetic acid were detected) on MTN-5, whereas acetic acid was formed at a yield close to 15% (whereas no acrylic acid was detected) over MS-2. In VPO-A, furan (not formed on MS-2 or on MTN-5 catalysts) and acetic acid were observed, although the selectivity never exceeded 5%. We discuss the formation of these compounds later, but note that both parallel and consecutive reactions occurred during the oxidation of 1-butene.

3.4. *FTIR of 1-butene adsorbed*

Butenes have been proposed as the reaction intermediates during the selective oxidation of *n*-butane to maleic anhydride on V–P–O catalysts [14,36,37]. Therefore, it could be interesting to follow a comparative FTIR study on the adsorption of 1-butene over some representative catalyst (i.e., MTN-5, MS-2, and VPO-5), to evaluate the possible reaction pathways during *n*-butane and 1-butene oxidation.

FTIR spectra of adsorbed 1-butene on the MTN-5 catalyst are shown in Fig. 5A. At 100 °C, strong IR bands can be seen at 1521, 1176, and 1168 cm^{-1}, which were previously observed

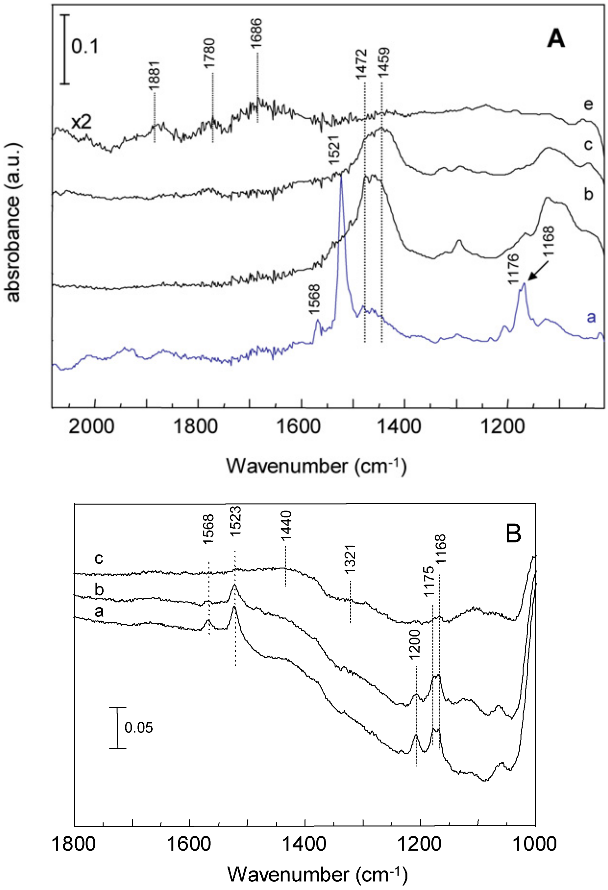

Fig. 5. (A) FTIR of 1-butene adsorption on MTN-5 catalyst at desorption temperatures of: (a) 100, (b) 200, (c) 350, and further co-adsorption of oxygen at 350 °C for 10 min (e), (B) FTIR of 1-butene adsorption on MS-2 catalyst at desorption temperatures of: (a) 100, (b) 150, and (c) 350 °C.

in the IR spectra of adsorption propylene [38] and attributed to the formation of enolic-type compounds. Along with these, other, less-intense bands appear at 1568 (associated with butadiene [39]), 1472, and 1459 cm^{-1}. The two latter bands, together with the shoulder at 1530 cm^{-1}, can be tentatively associated with furan species [39]. These emerged at 100 °C and increased at increasing temperature (150–350 °C), whereas the intensities of the IR bands associated with the enolate and butadiene-like species decreased at increasing desorption temperatures, suggesting that they must be intermediate species in the formation of the corresponding reaction products. Acrylate-type compounds (IR band at 1294 cm^{-1} [38]) can be clearly seen at 200 °C.

The addition of oxygen at 350 °C led to a complete disappearance of these bands associated with furan and enolate species and the appearance of new, less-intense IR bands at around 1881, 1780, and 1686 cm^{-1} associated with maleic anhydride and carbonyl species, respectively [40]. Thus, according to our IR results, enolate species together with butadiene were the first intermediates obtained during the oxidation of 1-butene on MTN-5. Moreover, these were transformed to carboxylic compounds, acrylate-type species, and maleic anhydride when the desorption temperature was increased up to 350 °C.

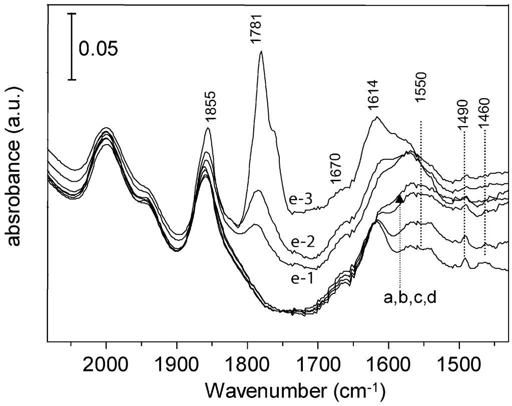

Fig. 6. FTIR of 1-butene adsorption on VPO-A catalyst at (a) 100, (b) 200, (c) 300, and (d) 350 °C, and further co-adsorption of oxygen at 350 °C for (e-1) 2, (e-2) 5, and (e-3) 10 min.

The IR spectra of adsorbed 1-butene on the MS-2 sample are shown in Fig. 5B. At a desorption temperature of 100 °C (Fig. 5B, spectrum a), strong bands at 1523, 1175, and 1168 cm^{-1} associated with enolic-type compounds can be seen, along with another intense IR band at 1567 cm^{-1} associated with butadiene. However, no bands at 1472 and 1459 cm^{-1} due to furan-type species can be seen. These results are similar to those observed on MTN-5. With increasing temperature, the bands due to butadiene and enolate-type species tended to disappear, whereas no band at 1297 cm^{-1} related to acrylate type species can be observed. After the addition of oxygen at 350 °C, no bands due to maleic anhydride were observed (1881 and 1780 cm^{-1}); only broad bands at 1440 and 1321 cm^{-1} related to carboxylic-type compounds were visible. Thus, according to our IR results, the same intermediate species (butadiene and enolic-type species) were observed in both the MTN-5 and MS-2 samples, whereas acrylate-type compounds were seen only in the MTN-5 sample.

For comparison, we also studied the adsorption of 1-butene on the VPO-A catalyst. Due to a strong IR adsorption in the region below 1300 cm^{-1}, the IR spectra were recorded only in the 4000–1430 cm^{-1} region. Fig. 6 shows the IR results obtained in the 2100–1100 cm^{-1} region. Adsorption of 1-butene at room temperature on the VPO catalyst led to the appearance of IR bands at 1550, 1490, and 1460 cm^{-1}, which can be assigned to surface-bound furan species [39,40], increased in intensity with increasing desorption temperature (100–350 °C). The addition of oxygen at 350 °C led to a diminution of the bands related to furan species (at 1550, 1490, and 1460 cm^{-1}) and the appearance of new IR bands at 1855 and 1781 cm^{-1} (due to maleic anhydride [39,40]) and at 1640, 1614, and 1574 cm^{-1}. The band at 1640 cm^{-1} can be related to carbonyl species, whereas the bands at 1614 and 1570 cm^{-1} should be related to adsorbed species with C=C bonds and carboxylate groups.

We also note that before 1-butene adsorption, a sharp band in the IR spectra of VPO-A catalyst was observed at 3688 cm^{-1} (spectrum not shown), assigned to the OH stretching of OH groups of P–OH [41]. This band shifted to 3444 cm^{-1} (broad band) after 1-butene adsorption and subsequent desorption at 100–200 °C, whereas a new band at 3516 cm^{-1} was formed at increasing temperatures (300–350 °C). The broad band at 3444 cm^{-1} should be related to OH groups interacted with 1-butene, whereas the band at 3516 cm^{-1} can be assigned to the formation of new reduced V^{4+}–OH species [42], because it disappeared after the addition of oxygen.

According to these results, furan was the main first intermediate species observed after 1-butene adsorption on VPO-A, and was further transformed into maleic anhydride in the presence of oxygen at 350 °C. In this way, as has been reported in the literature [39], V^{5+}=O species (which transform in a reversible path to V^{4+}–OH in the presence of butene and oxygen) are involved in the oxidation of 1-butene to maleic anhydride.

4. Discussion

4.1. *On the nature of crystalline phase*

Despite a lower selectivity to maleic anhydride compared with that of V–P–O catalysts, Te- or Sb-containing MoV-based catalysts have been shown to be as active and relatively selective to maleic anhydride during the partial oxidation of *n*-butane, and seem to be more active catalytic systems. Table 4 shows the catalytic activity for *n*-butane oxidation and the rate of maleic anhydride formation per unit mass per unit time (STY_{MA}) obtained during the oxidation of *n*-butane and 1-butene on the most representative catalysts. Both the catalytic activity for *n*-butane oxidation and the rate of formation of maleic anhydride per unit mass per unit time on a MoVTeNbO mixed-oxide catalyst such as MTN-5 can be 2–3 times higher than on a vanadyl pyrophosphate-based catalyst such as VPO-A (Table 4). For this reason, and although at the moment the MoV-containing catalysts studied here are less selective than V–P–O mixed oxides, these seem to be interesting catalytic systems for the partial oxidation of *n*-butane to maleic anhydride.

The presence of crystalline M1 phases (i.e., $Te_2M_{20}O_{57}$ or $(SbO)_2M_{20}O_{56}$) in the active Te- or Sb-containing catalysts (Fig. 1), lead us to conclude that this is the active and selective crystalline phase in MoV-oxidic bronze catalyst for *n*-butane oxidation, in agreement with those proposed for the partial oxidation of propane [22,25–33] and ethane [23,24]. V^{5+}–O–Mo pairs in phase M1, which have been suggested to be directly involved in the oxidative activation of propane [27,28,33], also must be involved in the oxidative activation of *n*-butane.

Table 4
Catalytic activity and rate of formation of maleic anhydride per unit of mass per unit time obtained during the oxidation of *n*-butane and 1-butene on some representative catalysts[a]

Catalyst	*n*-Butane oxidation[a]		1-Butene oxidation[b]	
	Catalytic activity[c]	STY_{MA}[d]	Catalytic activity[c]	STY_{MA}[d]
MVS	39.8	4.7	511	206
MTN-5	59.8	36.4	709	331
VPO-A	17.5	19.5	177	155

[a] Reaction conditions in *n*-butane oxidation as in Table 2, reaction temperature of 400 °C.

[b] Reaction conditions in 1-butene oxidation in text, reaction temperature of 400 °C.

[c] Catalytic activity in the oxidation of *n*-butane or 1-butene, in $g_{C4}\,h^{-1}\,kg_{cat}^{-1}$.

[d] Rate of formation of maleic anhydride per unit of mass per unit time (STY_{MA}), in $g_{MA}\,h^{-1}\,kg_{cat}^{-1}$.

Indeed, there is a parallelism between the catalyst performance in the oxidation of propylene to acrolein and in the oxidation of 1-butene to butadiene [43,44]. Therefore, the active sites present in M1-containing catalyst must play a similar role in the selective oxidation of propane/propylene and in *n*-butane/1-butene oxidation. Accordingly, as for the selective oxidation of propane to acrylic acid [27,28,33,45], the partial oxidation of *n*-butane on MoVTeNbO catalysts can be explained by the presence of three moieties: (i) activation of *n*-butane in V-sites, Mo–O–V–O–(Mo or Nb) like; (ii) oxidation of 1-butene to butadiene in Mo/Te sites, Te–O–Mo–O–(Te or V) like; and (iii) oxidation of butadiene to maleic anhydride in Mo/Nb sites, Nb–O–Mo–O–(Nb or V) like.

Nevertheless, the presence of Nb in both MoVTeO or MoVSbO seems to have a promoter effect, enhancing the selectivity to maleic anhydride (Table 2). This also was observed during the oxidation of propane to acrylic acid on similar catalysts [46].

4.2. *On the reaction network in n-butane oxidation*

The catalytic results on the oxidation of 1-butene and the IR results of 1-butene adsorption on V–P–O- and MoVTeNbO-type catalysts allows us to compare the reaction network and the nature of intermediates formed during *n*-butane oxidation over these catalysts. Scheme 1 shows the reaction network for *n*-butane oxidation on Nb-free and Nb-containing MoVTe(Sb)-based oxidic bronzes proposed from the results obtained during the oxidation of *n*-butane and 1-butene.

The formation of maleic anhydride on MoV-based catalysts is similar to that proposed for V–P–O catalysts [1–4]. In agreement with previously reported results [47], the ca. 70% selectivity to maleic anhydride during *n*-butane oxidation on the VPO catalyst (Fig. 2c) was higher than that achieved during 1-butene oxidation (ca. 50%; Fig. 4a). However, the opposite occurred on MTN-5, where the selectivity to maleic anhydride was higher for the oxidation of 1-butene (ca. 40%; Fig. 4a) than for *n*-butane (ca. 35%; Fig. 2b).

Another important difference between the catalytic performance of VPO catalysts such as VPO-A and MoVTeNbO catalysts such as MTN-5 is related to the selectivity to the main reaction products obtained during the oxidation of 1-butene. At low reaction temperature, VPO-A selectively transforms 1-butene to 2-butene, whereas MTN-5 or MS-2 are most effective in the transformation of 1-butene to butadiene (Figs. 4b and 4c). These results are related to the highest surface acidity of V–P–O catalysts [1–4] compared with the low or the moderate acidity observed for MoVTeNbO or MoVSbO mixed oxides [38,48]. Thus, the isomerization of 1-butene into *cis*- and *trans*-2-butene was favored over VPO-A, whereas the oxidative dehydrogenation of butenes to butadiene was favored over MS-2 or MTN-5.

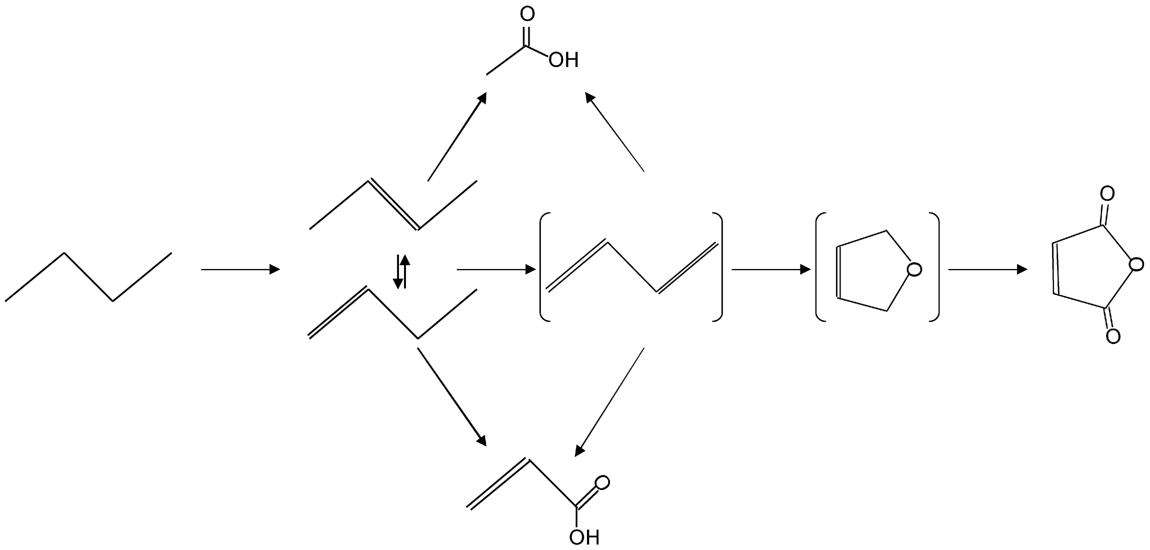

Scheme 1. Reaction network for *n*-butane oxidation on MoV-containing oxidic bronzes.

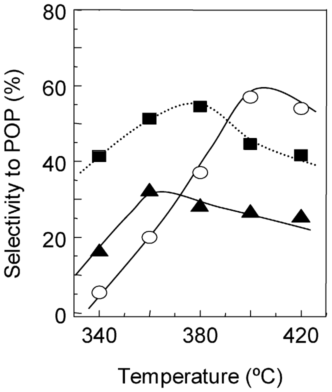

Fig. 7. Variation of the selectivity to partial oxidation products, POP (butadiene + maleic anhydride) with the reaction temperature obtained during the oxidation of 1-butene over (▲) MS-2, (■) MTN-5, and (○) VPO-A catalysts. Reaction conditions as Fig. 3.

Fig. 7 shows the variation of the selectivity to the partial oxidation products (butadiene and maleic anhydride) with the reaction temperature obtained during the oxidation of 1-butene on MS-2, MTN-5, and VPO-A. At low reaction temperature, MTN-5 was more selective to partial oxidation products than VPO-A, probably due to to its greater catalytic activity in the oxidation of 1-butene.

The in situ IR spectra of adsorbed 1-butene clearly showed more abundant formation of maleic anhydride adsorbed over VPO-A (Fig. 6) than on MTN-5 (Fig. 5), as evidenced by the much higher intensity of the corresponding bands at 350 °C and in the presence of molecular oxygen. Therefore, it is possible that the differences in the selectivity to maleic anhydride observed between both catalytic systems are partially related to the different performance in the oxidation of the olefin intermediates.

On the other hand, and according to the results of 1-butene oxidation, the formation of acrylic acid and acetic acid on MoVTeNbO (sample MTN-5) and on MoVSbO (sample MS-2) can be explained by the formation of other intermediates in addition to those related to the formation of maleic anhydride observed mainly on VPO-A catalysts. In this way, enolate-type species (which can be considered as the precursors of acrylic acid) are observed as the first intermediate species formed from 1-butene over MTN-5. For this reason, the formation of both acetic acid and acrylic acid as minor reaction products can be explained by the oxidative scission of C_4-olefins (1-butene, 2-butene, and butadiene), in agreement with previous results reported for the oxidation of Mo–V–O mixed oxides [49].

On the other hand, acetic acid is observed during the oxidation of 1-butene on sample MS-2. The relatively higher acidity of this with respect to that observed on MTN-5 [38,48] should favor partial isomerization of 1-butene to 2-butene, which is transformed into acetic acid by the oxidative scission of 2-butene.

It has been reported that activation of *n*-butane and 1-butene on V–P–O catalysts requires different active vanadium species [47]. V^{5+} species seem to be more appropriate for the olefin activation; V^{4+} cations, for alkane activation. Thus, the optimal phase for 1-butene oxidation to maleic anhydride has been reported to be β-$VOPO_4$ (V^{5+}), whereas $(VO)_2P_2O_7$ (V^{4+}) is the main crystalline phase in commercial catalysts for partial oxidation of *n*-butane.

At least two different activation sites for butane transformation can exist in Nb-free and Nb-containing MoVTe(Sb)-based oxidic bronze catalysts: Te–O–Mo or Sb–O–Mo pairs involved in the formation of butadiene and V^{5+} species involved in the formation of maleic anhydride from butenes. This fact can explain the different catalytic performance of MTN-5 and VPO-A catalysts in the oxidation of the alkane and the olefin. MTN-5, in which vanadium is present as V^{4+}/V^{5+} [50,51] but mainly as V^{5+} on the surface [27,28], should show a higher selectivity to maleic anhydride in the oxidation of 1-butene than in the oxidation of *n*-butane. Conversely, VPO-A, in which vanadium is present as $(VO)_2P_2O_7$ (as V^{4+} and on the surface as V^{5+}/V^{4+}, mainly V^{4+}), is more selective during the oxidation of *n*-butane, in agreement with previous results [1–4].

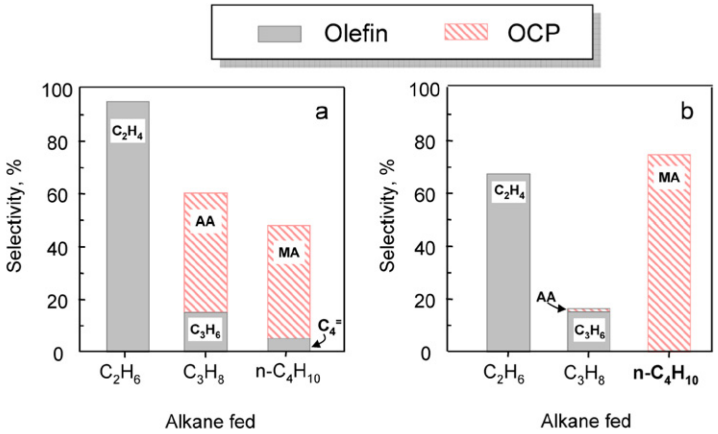

Fig. 8. Selectivity to olefins and O-containing partial oxidation products (OCP) obtained during the oxidation of ethane, propane and n-butane over (a) MTN-5 and (b) VPO-A catalysts. Reaction conditions: alkane/oxygen/helium = 4/8/88. Contact times selected to give an alkane conversion of ca. 25%; reaction temperature of 380 °C. Reaction products: (i) ethylene from ethane, (ii) propylene and acrylic acid (AA) from propane, (iii) C_4-butenes ($C_4^=$) and maleic anhydride (MA) from butane.

4.3. On the catalytic behavior of MoVTeNbO and VPO catalysts in alkane oxidation

V–P–O and MoVTeNbO mixed-metal oxide catalysts have been proposed to be active and selective for the partial oxidation of short-chain alkanes, although their catalytic performance changes depending on the alkane feed. Fig. 8 shows the comparative selectivity to partial oxidation products obtained during the oxidation of C_2–C_4 alkanes on MoVTeNbO (MTN-5) and V–P–O (VPO-A) catalysts. We note that whereas ethylene was the only partial oxidation product from ethane, propylene and acrylic acid were the main partial oxidation products obtained from propane and C_4 olefins and maleic anhydride were the main partial oxidation products obtained from n-butane.

For the MTN-5 catalyst, the selectivity to partial oxidation products decreased from ethane to butane (Fig. 8a). Considering the type of partial oxidation product, the selectivity to olefin decreased and the formation of O-containing partial oxidation products increased from ethane to butane. We note that these results were obtained in a steam-free feed, and the selectivity to acrylic acid is strongly enhanced in the presence of steam in the feed (ca. 70%) [52].

For the VPO-A catalyst, the selectivity to partial oxidation products was higher from ethane (with selectivity to ethylene of ca. 65%) and n-butane (with selectivity to maleic anhydride is ca. 75%) and lower from propane (with mainly propylene and only traces of acrylic acid) (Fig. 8b). This finding is in agreement with some previous results demonstrating that the catalysts most selective to maleic anhydride V–P–O (used after activation in n-butane/air) yielded only traces of acrylic acid [53,54].

Fig. 9 shows good correlation in the selectivity to acrylic acid and to maleic anhydride obtained during the oxidation of propane and n-butane, respectively, on MoV-based catalysts (at an alkane conversion of 20%). However, no correlation can be seen on an active and selective V–P–O catalyst such as VPO-A, suggesting that the quite different physicochemical characteristics are required for the oxidation of n-butane and propane in this catalyst.

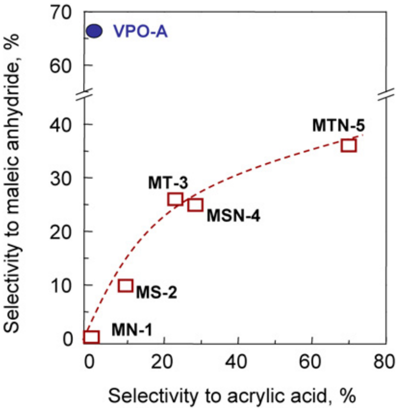

Fig. 9. Relationship between the selectivity to maleic anhydride obtained during the oxidation of n-butane and the selectivity to acrylic acid obtained during the oxidation of propane on MoV-containing mixed metal oxides and VPO-A catalysts. Reaction temperature = 380 °C; Alkane conversion = 20%. Reaction conditions of propane and n-butane oxidation and characteristics of catalysts as in Tables 1 and 2.

Recently, other authors have claimed a relatively high yield to acrylic acid during the oxidation of propane on V–P–O catalysts [7–9]. However, the catalyst activation procedure seems to be very different from those used in the activation of selective V–P–O catalysts for n-butane oxidation. Thus, it has been observed that it is possible to obtain acrylic acid from propane or maleic anhydride from n-butane using the same VPO catalyst precursor but submitted to different catalyst activation procedures, producing significantly modified physicochemical characteristics of the catalysts [7–9]. Thus, the activation of V–P–O catalysts used in the selective oxidation of propane must differ significantly from those used in the activation of VPO catalysts for n-butane oxidation.

According to the results presented herein, we can conclude that an advantage of MoV-containing multicomponent catalysts (especially MoVTe(Sb)NbO mixed oxides) with respect to V–P–O catalysts is that MoV-based catalysts can operate at a relatively high selectivity for different substrates without changes in the catalyst activation procedure. It also may be interesting to investigate whether it is possible to modify the characteristics of these catalysts to improve the selectivity in the partial oxidation of short-chain alkanes.

5. Conclusion

We have shown that MoVTe(Sb)NbO mixed-metal oxide catalysts are active and relatively selective during the oxidation of n-butane and 1-butene to maleic anhydride. Unfortunately, this catalytic system demonstrates important drawbacks compared with V–P–O catalysts, including lower selectivity to maleic anhydride and greater production of byproducts. But the productivity to maleic anhydride is ca. 2 times higher on MoV-oxidic bronze catalysts due to their higher catalytic activity, which has the additional advantage of easy activation (calcination in N_2 for 2 h) to be catalytically active and selective. Note that the higher activity of MoVTeNbO catalyst is not a consequence of its high surface area, because the VPO used in this work has a greater surface area.

Although only the systems presenting the M1 phase were found to be active and selective in the oxidative alkane activation, the catalytic behavior of MoV-containing oxidic bronze catalysts depends strongly on the catalyst composition. Thus, the M1 phase [i.e., $Te_2M_{20}O_{57}$ and $(SbO)_2M_{20}O_{56}$] in Te- and Sb-containing catalysts, respectively, is the active and selective crystalline phase for the activation of short-chain alkanes on these mixed-metal oxides. Furthermore, our results also suggest the possibility of tailoring catalytic behavior by changing the catalyst composition.

The active and selective MoVTeNbO catalyst used here has been previously optimized for the selective oxidation of propane to acrylic acid [27]. Although a correlation between both reactions has been observed for MoV-containing catalysts, this does not mean that these are the optimal catalysts in the selective oxidation of n-butane. In fact, VPO catalysts disrupt this trend (Fig. 9). Consequently, further improvement in the selectivity to maleic anhydride by modifying the surface/structural characteristics of these materials would be expected. A modification of surface active sites leading to lower reactivity and thus preventing the direct combustion of n-butane could be the way to obtain better catalytic performance. Along these lines, an initial modification of this catalyst could be the elimination of nonselective sites responsible for the formation of enolate-type intermediates, which seems to favor the formation of acrylic/acetic acid at low conversion and carbon oxides at high conversions of n-butane or 1-butene. Against the background of the present study, this catalytic system merits further investigation to establish the potential of these catalysts for the selective oxidation of n-butane to maleic anhydride.

Acknowledgments

Financial support was provided by the DGICYT (project PPQ2003-03946). B.S. thanks the M.E.C. (Ramón y Cajal Programme) for support.

References

[1] N. Ballarini, F. Cavani, C. Cortelli, S. Ligi, F. Pierelli, F. Trifiro, C. Fumagalli, G. Mazzoni, T. Monti, Top. Catal. 38 (2006) 147.
[2] G.J. Hutchings, J. Mater. Chem. 14 (23) (2004) 3385.
[3] G. Centi, F. Cavani, F. Trifiró, Selective Oxidation of Hydrocarbons, Kluwer Academic/Plenum, New York, 2001.
[4] G. Centi, Catal. Today 16 (1993).
[5] F. Cavani, F. Trifiro, Catal. Today 51 (1999) 561.
[6] G. Centi, J.M. López Nieto, D. Pinelli, F. Trifiró, Ind. Eng. Chem. Res. 28 (1989) 400.
[7] (a) G. Landi, L. Lisi, J.C. Volta, Chem. Commun. (2003) 492;
(b) G. Landi, L. Lisi, J.C. Volta, Catal. Today 91–92 (2004) 275.
[8] Y.H. Taufiq-Yap, C.S. Saw, R. Irmawati, Catal. Lett. 195 (2005) 103.
[9] X.K. Li, W.-J. Ji, J. Zhao, Z. Zhang, C.-T. Au, Appl. Catal. A Gen. 306 (2006) 8.
[10] M. Ai, J. Catal. 101 (1986) 389.
[11] Y. Han, H. Wang, H. Cheng, R. Lin, J. Deng, New J. Chem. (1998) 1175.
[12] B. Solsona, V.A. Zazhigalov, J.M. López Nieto, I.V. Bacherikova, E.A. Diyuk, Appl. Catal. A Gen. 249 (2003) 81.
[13] M. Loukah, G. Coudurier, J.C. Vedrine, M. Ziyad, Micropor. Mater. 4 (1995) 345.
[14] M.E. Davis, C.J. Dillon, J.H. Holles, J. Labinger, Angew. Chem. Int. Ed. 41 (5) (2002) 858.
[15] J.H. Holles, C.J. Dillon, J.A. Labinger, M.E. Davis, J. Catal. 218 (2003) 42.
[16] C.J. Dillon, J.H. Holles, R.J. Davis, J.A. Labinger, M.E. Davis, J. Catal. 218 (2003) 54.
[17] J.M. Galownia, A.P. Wight, A. Blanc, J.A. Labinger, M.E. Davis, J. Catal. 236 (2005) 356.
[18] (a) S. Albonetti, F. Cavani, F. Trifiró, Catal Rev. Sci. Eng. 38 (1996) 413;
(b) M.M. Lin, Appl. Catal. A Gen. 207 (2001) 1.
[19] H.X. Dai, C.T. Au, Curr. Top. Catal. 3 (2002) 33.
[20] T. Blasco, J.M. López Nieto, Appl. Catal. A Gen. 157 (1997) 117.
[21] T. Ushikubo, H. Nakamura, Y. Koyasu, S. Wajiki, US Patent 5,380,933, 1995; EP 0,608,838 B1, 1997.
[22] (a) T. Ushikubo, K. Oshima, A. Kayou, M. Hatano, Stud. Surf. Sci. Catal. 112 (1997) 473;
(b) T. Ushikubo, Catal. Today 78 (2003) 2003.
[23] J. López Nieto, P. Botella, M.I. Vázquez, A. Dejoz, Chem. Commun. (2002) 1906.
[24] P. Botella, E. García-González, A. Dejoz, J.M. López Nieto, M.I. Vázquez, J. González-Calbet, J. Catal. 225 (2004) 428.
[25] J.M. M Millet, H. Roussel, A. Pigamo, J.L. Dubois, J.C. Jumas, Appl. Catal. A Gen. 232 (2002) 77.
[26] J.M.M. Millet, M. Baca, A. Pigamo, D. Vitry, W. Ueda, J.L. Dubois, Appl. Catal. A Gen. 244 (2003) 359.
[27] P. Botella, J.M. López Nieto, B. Solsona, A. Mifsud, F. Marquez, J. Catal. 209 (2002) 445.
[28] R.K. Grasselli, J.D. Burrington, D.J. Buttrey, P. De Santo, C.G. Lugmair, A.F. Volpe, T. Weingard, Top. Catal. 23 (2003) 5.
[29] W. Ueda, K. Oshihara, D. Vitry, T. Hisano, Y. Kayashima, Catal. Surv. Jpn. 6 (2002) 33.
[30] H. Tsuji, K. Oshima, Y. Koyasu, Chem. Mater. 15 (2003) 2112.
[31] E. García-González, J.M. López Nieto, P. Botella, J.M. González-Calbet, Chem. Mater. 14 (2002) 4416.
[32] P. DeSanto, D.J. Buttrey, R.K. Grasselli, C.G. Lugmair, A.F. Volpe, B.H. Toby, T. Vogt, Z. Krist. 219 (2004) 152.
[33] Botella, E. García-González, J.M. López Nieto, J.M. González-Calbet, Solid State Sci. 7 (2005) 507.
[34] J.M. Oliver, J.M. López Nieto, P. Botella, A. Mifsud, Appl. Catal. A 257 (2004) 67.
[35] G. Landi, L. Lisi, J.C. Volta, J. Mol. Catal. A Chem. 222 (2004) 175.
[36] J. Ebner, V. Fraschetti, G. Centi, F. Trifiró, Chem. Rev. 88 (1988) 55.
[37] B. Hodnett, Catal. Rev. Sci. Eng. 27 (1985) 373.
[38] P. Concepción, P. Botella, J.M. López Nieto, Appl. Catal. A 278 (2004) 45.

[39] V.S. Escribano, G. Busca, V. Lorenzelli, J. Phys. Chem. 95 (1991) 5541.

[40] Z.-Y. Xue, G.L. Schrader, J. Catal. 184 (1999) 87.

[41] G. Centi, G. Golinelli, G. Busca, J. Phys. Chem. 94 (1990) 6813.

[42] G. Busca, G. Centi, F. Trifiró, V. Lorenzelli, J. Phys. Chem. 90 (1986) 1337.

[43] S. de Rossi, M. Lo Jacomo, M. Gardini, P. Porta, J. Catal. 146 (1994) 126.

[44] P. Forzatti, F. Trifiró, P.L. Villa, J. Catal. 55 (1978) 52.

[45] R.K. Grasselli, Top. Catal. 15 (2001) 93.

[46] D. Vitry, Y. Morikawa, J.L. Dubois, W. Ueda, Appl. Catal. A Gen. 251 (2003) 411.

[47] E. Bordes, Catal. Today 16 (1993) 27.

[48] M. Baca, A. Pigamo, J.L. Dubois, J.M.M. Millet, Catal. Commun. 6 (2005) 215.

[49] T. Seiyama, K. Nita, T. Mahehara, N. Yamazoe, Y. Takita, J. Catal. 49 (1977) 164.

[50] R.K. Grasselli, D.J. Buttrey, P. DeSanto, J.D. Burrington, C.G. Lugmair, A.F. Volpe Jr., T. Weingand, Catal. Today 91–92 (2004) 251.

[51] P. DeSanto, D.J. Buttrey, R.K. Grasselli, C.G. Lugmair, A.F. Volpe, B.H. Toby, T. Vogt, Top. Catal. 23 (2003) 23.

[52] J.M. Oliver, J.M. López Nieto, P. Botella, Catal. Today 96 (2004) 241.

[53] G. Centi, Catal. Lett. 22 (1993) 53.

[54] G. Centi, J.M. López Nieto, F. Trifiró, F. Ungarelli, Stud. Surf. Sci. Catal. 55 (1990) 635.